AD-763 101

INTEGRATED OPTICS. SEMIANNUAL TECHNICAL REPORT NUMBER 1

Sanjiv Kamath, et al

Hughes Research Laboratories

Prepared for:

Air Force Cambridge Research

January 1973

DISTRIBUTED BY:

NTIS

National Technical Information Service
U. S. DEPARTMENT OF COMMERCE
5285 Port Royal Road, Springfield Va. 22151

AFCRL-TR-73-0209

17

AD 763101

INTEGRATED OPTICS

BY

G. SANJIV KAMATH, RICHARD M. MADDEN,
OGDEN J. MARSH, AND AMNON YARIV

HUGHES RESEARCH LABORATORIES
3011 MALIBU CANYON ROAD
MALIBU, CALIFORNIA 90265

CONTRACT NO. F19628-72-C-0322

PROJECT NO. 2074

SEMIANNUAL TECHNICAL REPORT NO. 1

JANUARY 1973

CONTRACT MONITOR: FREEMAN D. SHEPHERD, JR.
SOLID STATE SCIENCE LABORATORY

Reproduced by
NATIONAL TECHNICAL
INFORMATION SERVICE
U S Department of Commerce
Springfield VA 22151

APPROVED FOR PUBLIC RELEASE; DISTRIBUTION UNLIMITED

Sponsored by
DEFENSE ADVANCED RESEARCH PROJECTS AGENCY
ARPA ORDER 2074

Monitored by
AIR FORCE CAMBRIDGE RESEARCH LABORATORIES
AIR FORCE SYSTEMS COMMAND
UNITED STATES AIR FORCE
BEDFORD, MASSACHUSETTS 01730

D D C
RECEIVED
JUL 19 1973
B

UNCLASSIFIED
Security Classification

DOCUMENT CONTROL DATA - R&D

(Security classification of title, body of abstract and indexing annotation must be entered when the overall report is classified)

1. ORIGINATING ACTIVITY *(Corporate author)* Hughes Research Laboratories 3011 Malibu Canyon Road Malibu, California 90265	2a. REPORT SECURITY CLASSIFICATION Unclassified 2b. GROUP

3. REPORT TITLE

INTEGRATED OPTIC TECHNOLOGY PROGRAM

4. DESCRIPTIVE NOTES *(Type of report and inclusive dates)*

Scientific Interim

5. AUTHOR(S) *(First name, middle initial, last name)*

G. Sanjiv Kamath, Richard M. Madden, Ogden J. Marsh, and Amnon Yariv

6. REPORT DATE January 1973	7a. TOTAL NO. OF PAGES ~~64~~ 58	7b. NO. OF REFS 14
8a. CONTRACT OR GRANT NO. ARPA Order No. 2074 F19628-72-C-0322 b. PROJECT, TASK, WORK UNIT NOS. 2074 n/a n/a c. DOD ELEMENT 61101E d. DOD SUBELEMENT n/a	9a. ORIGINATOR'S REPORT NUMBER(S) Semiannual Technical Report No. 1 9b. OTHER REPORT NO(S) *(Any other numbers that may be assigned this report)* AFCRL-TR-73-0209	

10. DISTRIBUTION STATEMENT

A - Approved for public release; distribution unlimited.

11. SUPPLEMENTARY NOTES This research was sponsored by the Defense Advanced Research Projects Agency	12. SPONSORING MILITARY ACTIVITY Air Force Cambridge Research Laboratories (LQ) L. G. Hanscom Field Bedford, Massachusetts 01730

13. ABSTRACT

Films of optical quality suitable for waveguide and optical device elements have been designed and growth processes developed for producing such films. Films with various compositions and thicknesses have been prepared by chemically depositing GaAs and $Ga_{(1-x)}Al_{(x)}As$ upon GaAlAs and GaAs. Film thicknesses from 2 to 17 μm and compositions from x = 0.02 to x = 0.25 ($Ga_{1-x}Al_xAs$) were obtained. Techniques for determining the Ga-to-Al ratio have been developed (i.e., photoluminescent determination of bandgap and electron microprobe analysis) as controls for meeting the design parameters. Device structures consisting of channel guides and directional couplers have been developed in GaAs using ion machining techniques.

DD FORM 1 NOV 65 1473

1a

UNCLASSIFIED
Security Classification

UNCLASSIFIED

Security Classification

14. KEY WORDS	LINK A		LINK B		LINK C	
	ROLE	WT	ROLE	WT	ROLE	WT
GaAs						
GaAlAs						
Epitaxy						
Integrated Optics						
Waveguides						

UNCLASSIFIED

Security Classification

ib

ARPA Order No. 2074

Program Code No. 3D10

Contractor: Hughes Aircraft Co.

Effective Date of Contract:
1 June 1972

Contract No. F19628-72-C-0322

Principal Investigator and Phone No.
Dr. Ogden J. Marsh/213 456-6411

AFCRL Project Scientist and Phone No.
Dr. Freeman D. Shepherd, Jr./617
861-2225

Contract Expiration Date:
30 November 1973

Qualified requestors may obtain additional copies from the Defense Documentation Center. All others should apply to the National Technical Information Service.

ACCESSION for

NTIS White Section ☑
DDC Buff Section ☐
UNANNOUNCED ☐
JUSTIFICATION .....

BY .....
DISTRIBUTION/AVAILABILITY CODES

Dist.	AVAIL. and/or SPECIAL	
A		

AFCRL-TR-73-0209

INTEGRATED OPTICS

by

G. Sanjiv Kamath, Richard M. Madden, Ogden J. March,
and Amnon Yariv

HUGHES RESEARCH LABORATORIES
3011 Malibu Canyon Road
Malibu, California 90265

Contract No. F19628-72-C-0322
Project No. 2074

Semiannual Technical Report No. 1

January 1973

Contract Monitor: Freeman D. Shepherd, Jr.
Solid State Science Laboratory

Approved for public release; distribution unlimited.

Sponsored by

DEFENSE ADVANCED RESEARCH PROJECTS AGENCY

ARPA ORDER 2074

Monitored by

AIR FORCE CAMBRIDGE RESEARCH LABORATORIES
AIR FORCE SYSTEMS COMMAND
UNITED STATES AIR FORCE
BEDFORD, MASSACHUSETTS 01730

D D C
RECEIVED
JUL 19 1973

ABSTRACT

Films of optical quality suitable for waveguide and optical device elements have been designed and growth processes developed for producing such films. Films with various compositions and thicknesses have been prepared by chemically depositing GaAs and $Ga_{(1-x)}Al_{(x)}As$ upon GaAlAs and GaAs. Film thicknesses from 2 to 17 μm and compositions from x = 0.02 to x = 0.25 ($Ga_{1-x}Al_xAs$) were obtained. Techniques for determining the Ga-to-Al ratio have been developed (i.e., photoluminescent determination of bandgap and electron microprobe analysis) as controls for meeting the design parameters. Device structures consisting of channel guides and directional couplers have been developed in GaAs using ion machining techniques.

TABLE OF CONTENTS

I	INTRODUCTION AND SUMMARY	1
II	DEFINITION OF EPILAYER MATERIAL AND STRUCTURE REQUIREMENTS	5
	A. Limits on GaAs Epilayer Impurity Concentrations	5
	B. Limits on Al Concentration in GaAs - $Ga_{1-x}Al_xAs$ Waveguides	8
III	MATERIAL GROWTH	11
	A. Vapor Epitaxy	11
	B. Solution Regrowth Epitaxy (GaAs, $Ga_{1-x}Al_xAs$)	15
IV	SEMICONDUCTOR FILM CHARACTERIZATION-PHOTOLUMINESCENCE MEASUREMENTS	33
V	DEVICE ELEMENTS — APPLICATION OF ION MICROMACHINING TO THE FABRICATION OF THREE-DIMENSIONAL OPTICAL WAVEGUIDES	37
VI	FUTURE PLANS	47
	REFERENCES	49
	APPENDIX	51

Preceding page blank

LIST OF ILLUSTRATIONS

Fig. 1. (GaAl)As Epilayer as Received 13

Fig. 2. (GaAs) Vapor Epilayer Grown on GaAlAs 13

Fig. 3. Cross Sectional View of Wafer Shown in Fig. 2 14

Fig. 4. Solubility Limit of As in Gallium Versus Temperature 17

Fig. 5. Variation of Al Concentration Through the Epilayer Film Versus Film Thickness 20

Fig. 6. Growth Rate, $d\lambda/dT$ and Percentage Change of Al Concentration 21

Fig. 7. Schematic Diagram of Horizontal Liquid Epilayer Growth System 23

Fig. 8. Photograph of the Horizontal Liquid Epilayer Growth System 24

Fig. 9. Photograph of the Graphite Boat in Which the Epitaxial Growth Occurs 27

Fig. 10. Photograph of the Surface of a (GaAl)As Film 31

Fig. 11. Deviation in Surface Flatness of the Film 31

Fig. 12. Photomicrograph of the Cleaved Edge of a Double Layer 32

Fig. 13. Diagram of Photoluminescence Measurement Setup 35

Fig. 14. Channel Waveguide Fabrication by Removal of Superfluous Sections of an Epilayer 38

Fig. 15. Schematic Diagram of the Duoplasmatron Ion Beam Sputtering System 40

Fig. 16. An Extreme Example of a Guide with Rough Walls and Top Surface 42

Preceding page blank

Fig. 17. Good Quality Channel Waveguide Fabricated by Using Holographically Prepared Mask and Ion Machining 42

Fig. 18. Directional Couplers Fabricated in GaAs 44

Fig. 19. Multimode Directional Coupler Fabricated by Ion Machining in a GaAs Epilayer 45

SECTION I

INTRODUCTION AND SUMMARY

The objectives of this contract are to study and analyze the propagation, attenuation and modulation of coherent optical waves in thin film waveguides, and in particular to study epitaxial semiconductor structures at a wavelength of 8500 A, to determine the parameters controlling the solution regrowth epitaxy of the $Ga_{1-x}Al_xAs$ system, to study the influence of the index discontinuity and semiconductor carrier concentration on optical properties, and to develop elementary optical device elements.

This report covers the first six months of work on this contract. The work has consisted of: (1) defining the requirements of both materials and structures for forming thin film waveguides, (2) growth of chemical vapor deposited films of GaAs on GaAlAs substrates, (3) construction of a liquid phase epitaxial growth system, (4) growth in this system of GaAs and $Ga_{1-x}Al_xAs$ upon GaAlAs and GaAs, (5) the development and completion of a photoluminescent test setup for the determination of the optical band gap in the GaAlAs epitaxial layers, (6) fabrication of channel guides and directional couplers in GaAs using ion micromachining techniques. The last task was partially Company supported but is described in this report for completeness. A summary of these accomplishments made during this work period are discussed in the following paragraphs.

1. Carrier Absorption and Guiding in Thin Film Waveguides:

Theoretical estimates of the expected losses in thin film semiconductor waveguides have been made. The result for GaAs is that the theoretical attenuation constant is given by

$$\alpha = (3.6 \times 10^{-19} N)\ \mathrm{cm}^{-1}$$

where N is the maximum carrier concentration in the structure (substrate or epitaxial layer). However, experimental data[1] suggest that this is a very optimistic estimate and a more realistic value is

$$\alpha \approx (10^{-17} N)\ \mathrm{cm}^{-1}$$

Deciding, at this point somewhat arbitrarily, that losses of $\alpha \leq 1\ \mathrm{cm}^{-1}$ can be tolerated, we obtain a criterion on the maximum allowable carrier concentration:

$$N < 10^{17}\ \mathrm{cm}^{-3}$$

We have calculated the aluminum concentration required in the substrate that has a GaAs epitaxial film on a $Ga_{1-x}Al_xAs$ substrate. For an epitaxial layer 2 μm thick, and at an optical wavelength of 1 μm, the minimum value for x (for guiding in the lowest order mode) is $x = 0.62 \times 10^{-2}$. However, the index discontinuity (and, therefore, the value of x), can increase by a factor of 9 before the next higher mode can be supported. Thus we estimate that a good experimental starting point is $x \approx 4 \times 10^{-2}$. This will allow lowest order mode confinement down to an epitaxial layer thickness of about 1 μm.

2. GaAs and GaAlAs Epilayer Growth

The vapor epi growth apparatus is fully operational, and several films (~4 μm thick) of GaAs with good reproducible characteristics have

already been obtained. A comparison of the films grown by the vapor and liquid epitaxial methods suggests that judicious use of these two techniques will give the best results for fabricating complex wave-guiding structures.

We concentrated our efforts during this work period on the design and construction of a horizontal solution regrowth epitaxial system and the growth of films in this system.

Calculations of desirable operating conditions for growing the films have been made. Using solubility data for As in the GaAs system and information on the influence of adding Al to the system available in the literature, desirable conditions for the growth of epi films have been deduced. Because of the conflicting demands arising from considerations of film thickness, the homogeneity of doping level through the film cross-section and the very high segregation coefficient of Al in the system, the solution used for growth was a compromise. The actual operational parameters of interest are the temperature of the melt at the start of growth, the cooling rate and total cooling time, and the composition of the melt at the start.

Initial growth experiments were performed with growth of GaAs films on GaAs substrates. Later, films of GaAlAs were grown on GaAs and GaAlAs substrates. These films were grown with various compositions and thicknesses in order to ascertain control capability of the system. Film thicknesses from 2 to 17 μm were obtained and compositions from $x = 0.02$ to $x = 0.25$ ($Ga_{1-x}Al_xAs$) were established through microprobe analysis.

3. Photoluminescent Bandgap Measurements:

We intend to use photoluminescence measurements to analyze the quality of GaAs and $Ga_{(1-x)}Al_xAs$ epitaxial layers and the ratio of Ga/Al in the $Ga_{(1-x)}Al_xAs$. An experimental setup has been assembled for measuring the photoluminescence spectra of these materials. The optical pumping source is a 100 mw He-Ne laser with an output wavelength of 6328Å. The samples are held in a vacuum dewar on the cold

surface of a liquid nitrogen cryostat so that they can be cooled to 77°K if desired. Light emitted from the sample is collected by a lens and focused onto the slit of a Jarrell Ash 1/4 meter grating spectrometer. The detector is a 7102 photomultiplier tube, which is cooled to reduce noise. It remains to test the apparatus by measuring the characteristics of some standard samples.

4. Fabrication of Three-Dimensional Optical Waveguides by Ion Micromachining

Experiments were carried out on determining the suitability of ion milling in fabricating three-dimensional ridge waveguides as well as optical directional couplers. These techniques should play an important role in the latter part of the program when integrated optics components will be fabricated. One millimeter long guides with 3 x 7 μm and 1.4 x 2 μm cross-sections have been fabricated by ion sputtering using masks prepared by holographic techniques. Directional couplers were fabricated by partial removal of the epilayer between the guides using ion micromachining.

SECTION II

DEFINITION OF EPILAYER MATERIAL AND STRUCTURE REQUIREMENTS

A. LIMITS ON GaAs EPILAYER IMPURITY CONCENTRATIONS

Before undertaking the problem of GaAlAs epitaxial waveguide fabrication we need to understand the nature of the loss mechanisms which will attenuate the propagating mode. Relating these mechanisms to material parameters and incorporating guide propagation considerations will allow us to develop guidelines for waveguide fabrication. The most important sources of loss are: (1) band-to-band transitions and (2) free carrier absorption. Loss caused by the first mechanism can be minimized by a proper choice of the energy gap relative to the operating wavelength. Free carrier loss will be present, however, since the impurity concentration, although kept to a minimum, is always finite.

In an effort to determine the allowable impurity concentrations we need to solve for the optical losses of the propagating modes as a function of the carrier concentrations in the substrate and the guiding layer. Consider a thin film waveguide such as illustrated below.

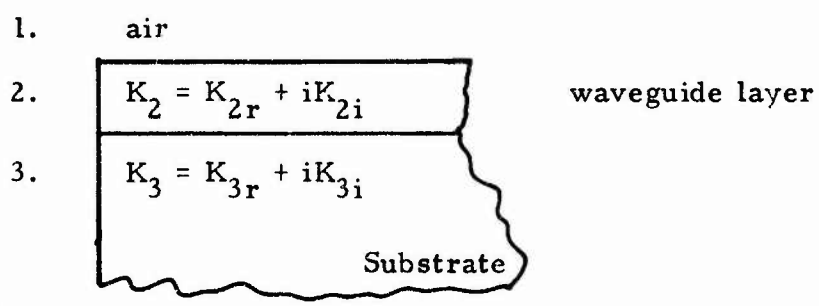

where K_1, K_2, and K_3 are the relative dielectric constants (i.e. $K = n^2$ with n being the complex index of refraction). The fact that the media are in general lossy is accounted for by taking the K's as complex

numbers as shown in the figure. Near cutoff most of the wave energy is in medium 3 and the mode attenuation approaches the bulk loss of medium 3 which is

$$\alpha_3 = \frac{k_o K_{3i}}{\sqrt{K_{3r}}} \tag{1}$$

where $k_o = \frac{2\pi}{\lambda_o}$. Far above cutoff the mode energy is concentrated in medium 2 and the mode loss approaches

$$\alpha_2 = \frac{k_o K_{2i}}{\sqrt{K_{2r}}} \tag{2}$$

We can obtain a general expression for the mode attenuation constant as a function of K_{2i}, K_{3i}, the guide dimensions and the frequencies. Such an expression has, indeed, been derived. As expected the mode loss constant lies between α_2 and α_3. For the purpose of design criteria we assume, conservatively, that the loss constant is equal to the larger of α_2 and α_3, i.e.,

$$\alpha_{mode} = \frac{k_o \ \mathrm{Im}K}{\sqrt{\mathrm{Re}K}}$$

where the imaginary part of K (ImK) is taken as the larger of $\mathrm{Im}K_2$ and $\mathrm{Im}K_3$.

An expression for ImK can be derived from a simple treatment of the carrier polarization in the presence of collisions of lifetime τ. This gives (see Appendix)

$$\mathrm{Im}K = - \frac{Ne^2 / \left(m^* \epsilon_o \omega\tau\right)}{\omega^2 + 1/\tau^2} \tag{3}$$

where m^* = effective mass, ϵ_o = dielectric constant of vacuum in MKS units and N = carrier density.

In GaAs using a mobility $\mu = 8.5 \times 10^3 cm^2/volt\ sec$ we have at $\lambda_o = 1\ \mu m$

$$m^* = 0.07\ m_e = 6.4 \times 10^{-32} Kg$$

$$\tau = \frac{m^* \mu}{e} = 3.4 \times 10^{-13}\ sec$$

$$\omega = 2\pi f \cong 1.88 \times 10^{15}$$

$$\omega\tau = 6.4 \times 10^2$$

$$n = 3.51$$

From eq. (2) and (3) we obtain in the limit $\omega >> 1/\tau$

$$\alpha_{mode} \doteq \sqrt{\frac{\mu_o}{\epsilon}}\ \frac{Ne^2}{m^* \omega^2 \tau} \tag{4}$$

where

μ_o = permeability of free space

ϵ = dielectric constant of the material

With the above data for GaAs we obtain

$$\alpha = 3.6 \times 10^{-19}\ N\left(cm^{-1}\right) \tag{5}$$

where N is in cm^{-3}.

In integrated optical circuits with typical dimensions of a few millimeters we should be able to tolerate $N < 10^{19}\ cm^{-3}$ at which point the loss in 1 mm should be $1-e^{-0.36} \approx 0.30$. As a hedge against unforeseen factors and the fact that experimental absorption[1] invariably runs higher than the value given by (5) we adopt the value

$$N \leq 10^{17}\ cm^{-3}$$

as a design parameter for the maximum carrier concentration in the substrate or the guiding layer.

B. LIMITS ON Al CONCENTRATION IN GaAl - $Ga_{1-x}Al_xAs$ WAVEGUIDES

The problem here is to determine the limits of the aluminum molar fraction x in $Ga_{1-x}Al_xAs$ such as to give single mode propagation in waveguides of reasonable dimensions.

The condition for propagation of the first m modes in a waveguide of height t is

$$2n(n_2 - n_3) > \left(\frac{m\lambda_o}{4t}\right)^2;\ m = 1, 3, 5 \ldots . \qquad (6)$$

The mode designation m = 1, 3, 5 .... is inherited from that of symmetric waveguide. The mode m = 1 is the lowest order propagating mode in the waveguide of Fig. 1 while m = 3 is the next higher mode. The even modes m = 0 and m = 2 which exist in a symmetric guide do not exist in our guide.

We anticipate that it is reasonable to operate our waveguides with heights t near a wavelength although eventual deviations by an order of magnitude either way can be envisaged. If we choose a smaller height then it becomes impossible to couple to the mode by an end-on incidence while if we go to $t \gg \lambda$ the advantages of waveguiding disappear.

Choosing thus $t = 2\ \mu m$ in eq. (6) and taking $\lambda_o = 1\ \mu m$, the condition for propagation of at least the lowest order mode ($m = 1$) is

$$n_2 - n_3 > \frac{1}{32n} \times \left(\frac{1}{2}\right)^2 \approx \frac{1}{400} \tag{7}$$

For GaAlAs, experience obtained in the close confinement injection lasers indicates that the index difference caused by adding aluminum to GaAs is

$$n_2 - n_3 \approx 0.4x \tag{8}$$

where x is the molar fraction of the aluminum.

If our waveguide is to support only the $m = 1$ (lowest order) mode, it follows from (6) that

$$9\left(\frac{\lambda_o}{4t}\right)^2 > 2\,(n_2 - n_3)\,n > \left(\frac{\lambda_o}{4t}\right)^2, \tag{9}$$

which for $t = 2\ \mu m$, $\lambda_o = 1\ \mu m$ and using (8) becomes

$$6 \times 10^{-2} > x > 6.25 \times 10^{-3}.$$

We choose as a design criterion $x = 4\%$ in order to stay comfortably within the allowed range.

The summary of our design criteria for low loss single mode waveguides is given below

Waveguide Height	Imp concentration for $\alpha < 1\,cm^{-1}$	Aluminum mole fraction
$t = 2\ \mu m$	$N < 10^{17}\,cm^{-3}$	$0.6\% < x \leq 4\%$

SECTION III

MATERIAL GROWTH

Two parallel approaches, vapor and liquid epitaxy, were used to form gallium arsenide structures suitable for waveguide applications. The objective was to form multilayer structures of varying compositions to provide refractive index discontinuities necessary for waveguiding. The two areas are discussed in detail in the sections below.

A. VAPOR EPITAXY

The primary emphasis in this part of the program was to form simple structures of gallium arsenide layers on gallium-aluminum-arsenide, GaAlAs, that could be used for preliminary studies based on our theoretical analysis of waveguide structures. The vapor deposition system already in use on other programs in the laboratory was used for growing these films.

The GaAlAs substrates were obtained from Laser Diodes, Inc., Metuchen, New Jersey. They were epitaxial layers of GaAlAs on GaAs substrates with composition $Ga_{0.96}Al_{0.04}As$ and a film thickness of about 12 microns. The surfaces were given a light chemical polish before being loaded into the growth apparatus. A brief description of our vapor growth system is given below.

Epitaxial layers of gallium arsenide are grown in an all-glass system using five-nine's arsenic trichloride and six-nines gallium with a flowing atmosphere of pure hydrogen supplied by a palladium diffusion purifier. The hydrogen is bubbled through arsenic trichloride, passed over gallium kept at about 850°C and subsequently over a gallium arsenide seed located downstream at about 780°C. The growth system has been used routinely in our laboratory to produce epitaxial layers with thickness larger than 5 microns and carrier concentrations in the range of 5×10^{16} cm^{-3}.

Preceding page blank

In a series of experiments we have used the system for growing gallium arsenide films on gallium aluminum arsenide. The system and control, however, are not quite adequate to grow films thinner than 4 microns reproducibly. When the films are thin, the thickness uniformity over the entire surface becomes a critical consideration, especially for use in waveguides. The film thickness is strongly dependent on the uniformity of the temperature across the whole cross section of the growth chamber where the seed is located. Besides uniformity in temperature, uniformity in the concentration of the gas phase at the growth front is also critical in producing a good junction at the growth interface. With these considerations in mind we have designed a new system on a company funded program incorporating more sophisticated controls. This will be used in our future experiments to provide thin films with a high degree of homogeneity and good surface finish.

Several films of gallium arsenide using the present system have been grown, however, to familiarize ourselves with the problems involved. A cross section of one such film is shown in Fig. 3. Also shown (in Figs. 1 and 2) are the surface of the gallium aluminum arsenide as received and the gallium arsenide film after growth. The layer is being presently investigated for its optical quality. It can be seen from the figures that the polishing of the GaAlAs substrate and the procedures used in the growth system are capable of giving a very good layer of GaAs with good perfection and junction delineation. The vapor growth method would thus seem to be an excellent tool to grow a layer of GaAs on GaAlAs.

Unfortunately, vapor-phase epitaxy has disadvantages when applied to growth of $Ga_{1-x}Al_xAs$ films. Because of the highly reactive nature of aluminum, it is extremely difficult to grow epilayers of GaAs with aluminum as an additive by the vapor epitaxial process. However, liquid epitaxial growth is ideally suited for GaAlAs film growth because the condensed phase eliminates many of the disadvantages that the vapor phase has. We also find that aluminum addition to gallium tends to lower the gallium surface tension causing good wetting of the substrate

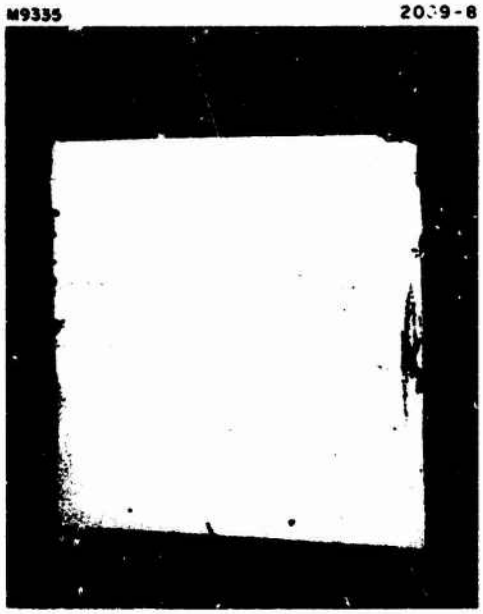

Fig. 1.
(GaAl)As Epilayer as Received

Fig. 2.
(GaAs) Vapor Epilayer Grown on GaAlAs.

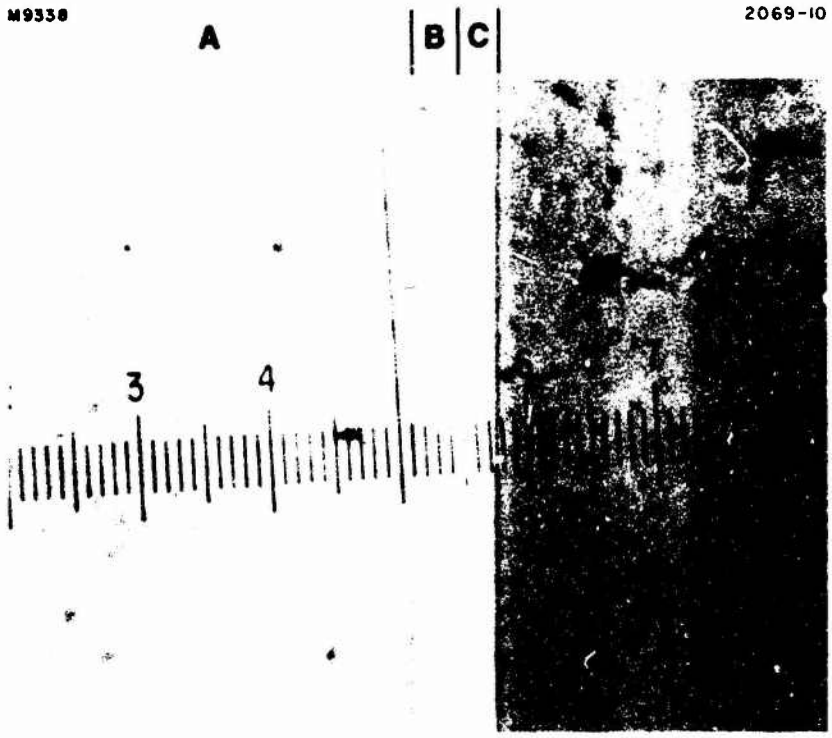

Fig. 3. Cross Sectional View of Wafer Shown in Fig. 2. Region A — GaAs Substrate. Region B — GaAlAs Epilayer (∿8.5 μ). Region C — GaAs Layer Grown by Vapor Epitaxy (∿5.5 μ).

surface, enabling very good growth of GaAlAs on GaAs. A further advantage is to be gained by using the liquid epitaxial method because aluminum has a high segregation coefficient during growth that enables the utilization of very dilute solutions of Al; for example, a 0.05% solution of Al in Ga under appropriate conditions will give a GaAlAs layer with 2% Al in the epi layer. This low concentration of the solution minimizes the problems caused by the high reactivity of aluminum, especially in the presence of traces of oxygen and water vapor.

It would seem from the above discussion that the judicious use of vapor and liquid epitaxial methods for producing complex waveguiding structures would give the best results. We hope to develop both these approaches to enable us to achieve this goal. In the sections below we give a detailed account of our work in the liquid epitaxial growth effort.

B. SOLUTION REGROWTH EPITAXY (GaAs, $Ga_{1-x}Al_xAs$)

A horizontal, open tube growth system has been designed, constructed and utilized to produce epitaxial films of GaAs and (GaAl)As. The following sections describe the growth concepts, system design, and properties of films grown to date.

1. Growth Method

The method of crystal growth in which a solid crystallizes in equilibrium with a dilute solution at a temperature below the melting point of the solid is referred to as solution regrowth. When the technique is applied to the growth of thin single crystal films on seed crystals it is often called liquid phase epitaxy. This is one of our approaches to the problem of fabricating optical guiding structures which will respond to the application of external fields and will transmit light with low losses at a wavelength of 8500Å.

The solvent material is high purity gallium which is liquid at growth temperatures of 850 to 950° C.

The first films grown in this program by this method were GaAs homo-junctions. The growth of GaAs films involves an initial saturation of gallium solvent with GaAs at the starting temperature and a subsequent cooling which results in supersaturation and precipitation of GaAs on the substrate as an epitaxial layer.

The solubility limit of arsenic in gallium versus temperature has been determined experimentally by R. N. Hall[2] and is depicted graphically in Fig. 4. Also shown in this figure are points corresponding to an analytical expression we have fitted to the experimental curve:

$$x^{\ell}_{GaAs} = (6 \times 10^{-2}) \times 10^{\{3.71 \times 10^{-3}(T-900) - 6.0 \times 10^{-6}(T-900)^2\}} \tag{10}$$

where x^{ℓ} = atom fraction of GaAs in liquid gallium and T is the temperature of the melt in ^{o}C. Notice that over the temperature range $500^{o}C$ - $1100^{o}C$ the analytical expression corresponds well to the experimental data. From the equation we can establish the relevance of several parameters to controlled thin film growth thus evaluating dx/dT near $900^{o}C$ yields

$$\left[\frac{dx^{\ell}_{GaAs}}{dT}\right] 900^{o}C \approx 5.13 \times 10^{-4}/^{o}C \ . \tag{11}$$

From eq. (11), for a system for which the kinetics are not diffusion limited, we can determine the film thickness produced by an incremental reduction in temperature near $900^{o}C$ under the assumptions that nucleation occurs only at the substrate in a uniform layer and no super cooling takes place. The change in film thickness (λ) with temperature is

$$\frac{d\lambda}{dT} = \frac{dx^{1}_{GaAs}}{dT} \frac{M_{GaAs}}{M_{Ga}} \frac{W_{melt}}{\rho_{GaAs} A} = -2\left(\frac{W_{melt}}{A}\right) \mu m/^{o}C \tag{12}$$

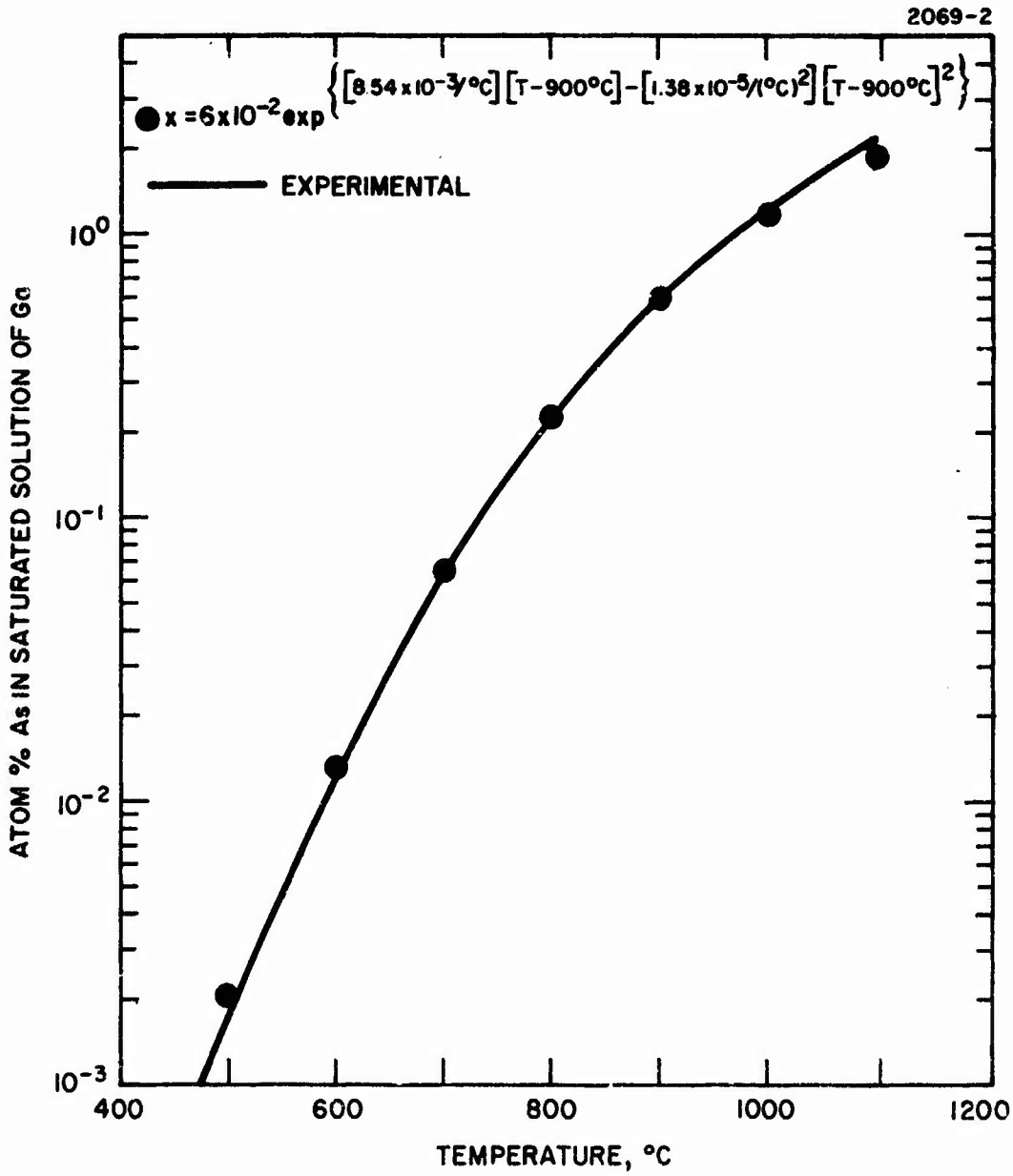

Fig. 4. Solubility Limit of As in Gallium Versus Temperature.

where

M_{GaAs} = Molecular weight of GaAs

M_{Ga} = Atomic weight of Ga

ρ_{GaAs} = Density of GaAs in gm/cm^3

W_{melt} = Weight of the melt in gm

A = Area of the substrate in cm^2 .

In our experiments a typical ratio of melt weight to substrate area is about 1 gm/cm^2. This implies a growth rate of 2 $\mu m/^oC$. It is clear from this that reproducibility in thickness requires fine temperature control.

The second phase of the growth program involves the growth of $Ga_{1-x}Al_xAs$ on GaAs. The solubility of GaAs in the gallium melt should not be significantly affected by the addition of a small amount of Al to the melt but a new consideration arises regarding the uniformity of the Al concentration throughout the grown layer. Consider the mixed GaAs-AlAs system, AB, where A designates cations on an f. c. c. lattice and B designates anions on the other sublattice comprising the zinc blende structure. Near 900^oC the "A" site fraction of Al in solid AB at equilibrium with a gallium rich melt is about 58 (Ref. 3) times the atom fraction of Al in the melt. Consequently, as the film grows it quickly depletes the melt of Al. Again assuming uniform nucleation on the substrate and nowhere else, it can be shown that

$$\frac{d\ln x_{Al}^{A}(\text{interface})}{d\lambda} \approx -58\left(\frac{M_{Ga}}{M_{GaAs}}\right)\rho_{GaAs}\left(\frac{A}{W_{Melt}}\right) \qquad (13)$$

where x_{Al}^{A} (interface) = site fraction of Al on the "A" lattice at the growth interface

The solution to this equation is, of course

$$x_{Al}^{A}\,(\text{interface}) \approx x_{Al}^{A,o}\ \exp\left[-58\left(\frac{M_{Ga}}{M_{GaAs}}\right)\rho_{GaAs}\left(\frac{A}{W_{melt}}\right)\right] \qquad (14)$$

where $x_{Al}^{A,o}$ = Al site fraction on the "A" lattice at the initiation of growth.

Figure 5 shows the percentage deviation of the Al site fraction on the "A" lattice at the surface of the film to its value at the substrate-epi junction as a function of film thickness for various values of the parameter (W_{melt}/A). Clearly large ratios of (W_{melt}/A) correspond to more uniform film composition.

It would seem from the above argument that (W_{melt}/A) should be kept large. Doing this produces another problem. When thin films are desired, however, eq. (12) indicates that the film thickness produced through a given cooling increment is directly proportional to (W_{melt}/A). Conversely, the total cooling increment, ΔT, required to grow a film of a given thickness is inversely proportional to (W_{melt}/A). Since there are limits to how well the temperature can be controlled, large ratios of (W_{melt}/A) reduce control over final film thickness. Problems associated with super cooling further complicate the situation. The discussion above leads to the conclusion that for best results a judicious compromise has to be used in choosing values of W_{melt}/A, depending on the thickness of the film desired and the Al concentration gradient that can be tolerated in the film. It also emphasizes the high degree of sophistication necessary in the control of temperature both at the start of growth and during the cooling cycle. These considerations are seen in better perspective in the treatment below.

Figure 6 illustrates the dependence of growth rate and the derivative of the logarithm of Al concentration with respect to film thickness (eq. (13) on (W_{melt}/A). Film specifications restrict growth to particular regions of the figure. For instance, suppose a 10 μm thick film is

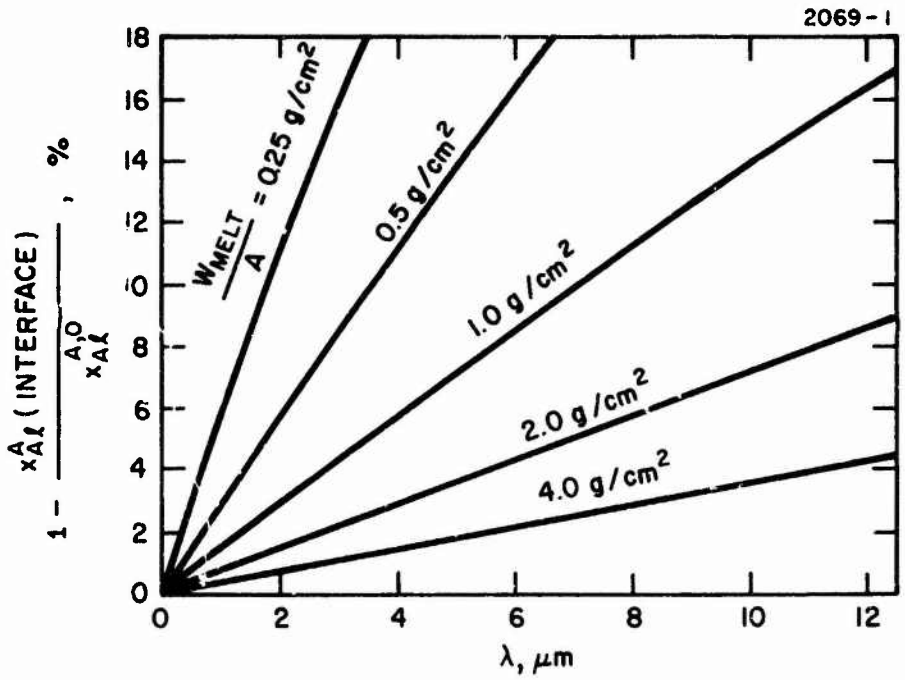

Fig. 5. Variation of Al Concentration through the Epilayer Film Versus Film Thickness for Particular Values of the Parameter W_{melt}/A.

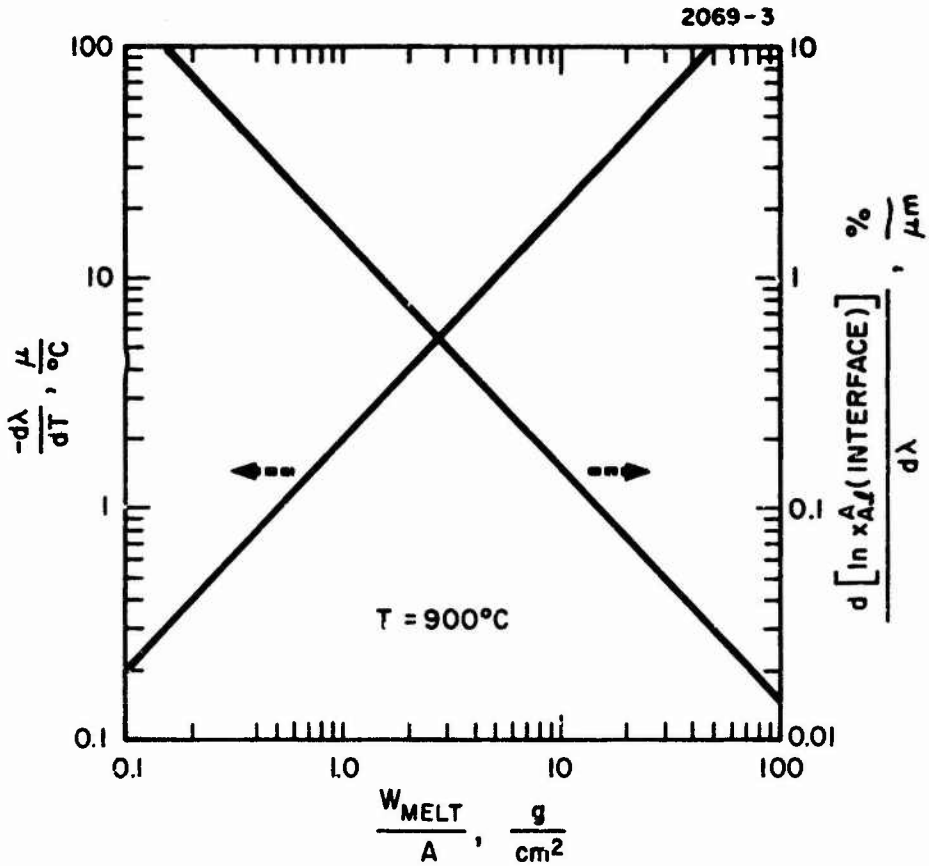

Fig. 6. Growth Rate, $d\lambda/dT$ and Percentage Change of Al Concentration for an Incremental Change in Film Thickness Versus W_{melt}/A.

required with a maximum allowable error in thickness of ±2%. If the uncertainty in the growth temperature is ±0.1% the growth rate must be less than 2 μm/°C to satisfy the requirement on film thickness. This limits the choice of (W_{melt}/A) to values less than 1 gm/cm^2. Figure 6 shows that under these conditions the variation in Al site fraction from substrate to surface of film will be 15%. To improve control over uniformity, one must pay a price in control of thickness and vice versa.

It should be emphasized that the description of the growth process given above is based on an over-simplified model. The assumptions of chemical uniformity throughout the melt, lack of super saturation and heterogeneous nucleation occurring only on the substrate are all unrealistic, but the simple model helps clarify general principles underlying the growth process. Equations (12) and (13) should be regarded only as guides illustrating the general dependence of the growth conditions on the various important parameters. Fortunately the model is especially applicable to our epitaxial growth system where the melt is of limited volume and has a small thickness above the substrate. This allows near equilibrium conditions to be established at the growth interface and minimizes effects of diffusion of various species. The growth rate predicted in eq. (12), for instance, is only about 3 times higher than that obtained in the horizontal system using 1 gm of melt with 1 cm^2 substrate area.

2. Epitaxial Growth Apparatus

The design of the furnace and gas handling equipment is shown schematically in Fig. 7. Figure 8 is a photograph of this apparatus. The system is constructed primarily of quartz, pyrex, and stainless steel, with short sections of kovar tubing used to make the transition from pyrex to stainless and a limited number of compression fittings. The only compression fittings used on the gas input side of the furnace tube are at the stainless steel nitrogen regulator and at the Ag-Pd diffuser output.

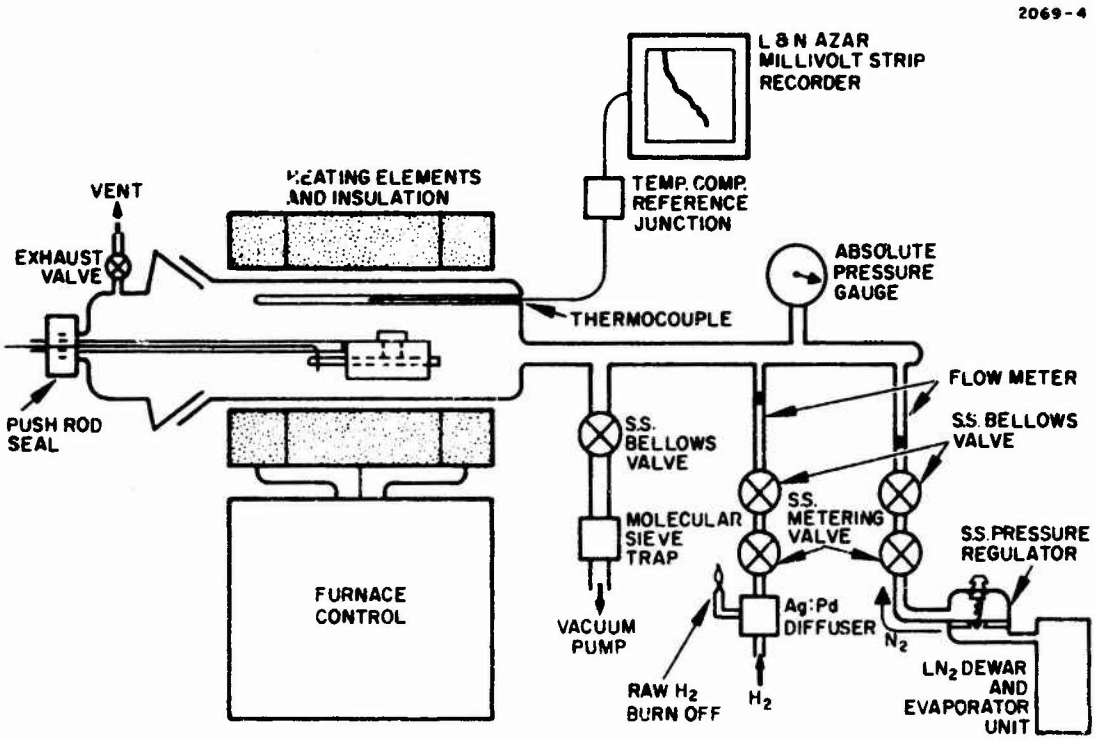

Fig. 7. Schematic Diagram of Horizontal Liquid Epilayer Growth System.

M9263

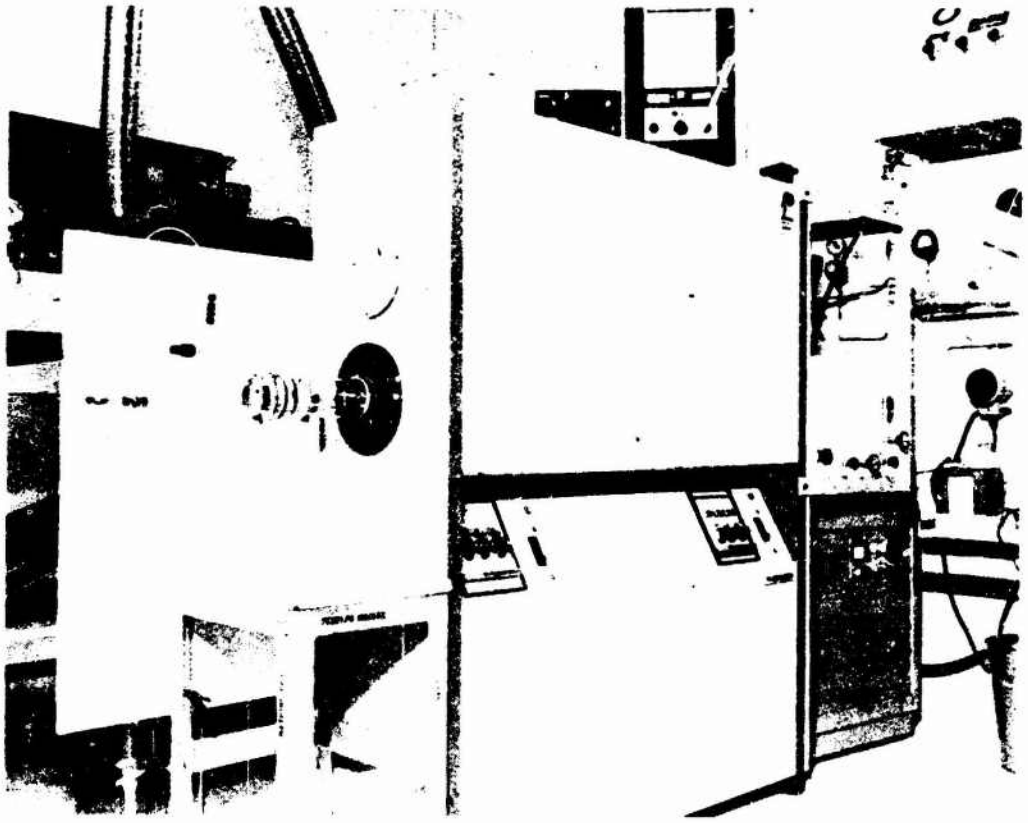

Fig. 8. Photograph of the Horizontal Liquid Epilayer Growth System.

The gaseous nitrogen source is the vapor over liquid nitrogen which ensures high purity without the necessity of a cold trap.

At the beginning of each run the system is evacuated using a Balzer mechanical vacuum pump which employs a bakeable molecular sieve trap to prevent back streaming of pump vapors. Stainless steel vacuum bellows valves isolate the gas sources from the vacuum pump during evacuation and serve as "on-off" valves to control the gas flows. The pressure reached during pump down measured between the molecular sieve trap and the vacuum pump is less than 10^{-3} Torr. This pressure is continuously monitored with a thermocouple gauge.

After evacuation the system is back filled with either H_2 or N_2. To monitor the manifold pressure during back filling a Wallace-Tiernan absolute pressure gauge is used. The chamber exhaust goes through a 3 pound check valve and a bath of silicone oil to prevent oxygen backstreaming.

The furnace itself is a Thermco "Spartans" diffusion furnace having 3 temperature zones which are controlled by a master-slave, 4 thermocouple control loop. This type of control system is ideal for maintaining a long, flat temperature profile even during cooling. The maximum furnace cooling rate measured in the thermocouple well is about $9^{o}C$/min with low gas flow.

The temperature during growth is monitored in a thermocouple well adjacent to the boat. The thermocouple E. M. F. is applied to a Leeds and Northrup millivolt recorder in series with a temperature compensated reference (cold) junction. This recorder is capable of displaying a 2 millivolt full scale span atop a calibrated d. c. level of up to 40 m. v. Finer temperature sensitivity is possible using a 5 digit digital voltmeter with 1 μ volt resolution. This permits measurements of temperature change as small as $0.1^{o}C$ using a Pt - Pt: Rh(13%) thermocouple. We find it possible to maintain a temperature which is constant to $\pm 0.1^{o}C$ in the growth zone of our system.

The boat containing the substrate and the melt is made of high purity graphite purchased from Ultra Carbon Corp. It consists of

2 pieces: the main body of the boat containing the melt which is covered with a graphite cap and a plate which slides through the center of the main body directly under and in contact with the melt. The sliding plate has two machined depressions which accept a GaAs source piece and the substrate. During growth the source piece is placed in contact with the melt by moving the sliding plate with respect to the boat body. This saturates the melt at the starting temperature. The substrate is shifted into contact with the melt just before cooling begins. Figure 9 is a photograph of the boat.

The two-section boat is controlled by a double push-rod having a concentric design. The outer rod is quartz and holds the main body of the melt in position. The inner rod is tungsten and attaches to the sliding plate.

3. Progress in Film Growth

After the epitaxial system was completed it was checked out by growing films of GaAs on silicon doped GaAs substrates (10^{18} electrons/cm^3). These films are n-type as grown, which is expected since the gallium melt was saturated using silicon-doped GaAs. The growth orientation was <100>.

These initial runs were helpful in pointing out problems inherent to the system. One difficulty, the complete removal of the melt from the film after growth, still has not been satisfactorily resolved in the present system especially while growing GaAs films. Careful attention to the spacing between the graphite wiping edge and the film surface and the incorporation of a second cavity in the graphite boat to provide additional wiping has helped to reduce the problem, but the resultant surface is too rough to permit photo-lithography without subsequent polishing. Final pol shing appears to be an acceptable solution only for films which are thicker than about 10 μm.

Fortunately it has proven much easier to remove the melt after growing a (GaAl)As film. The same growth apparatus yields surfaces

M9262

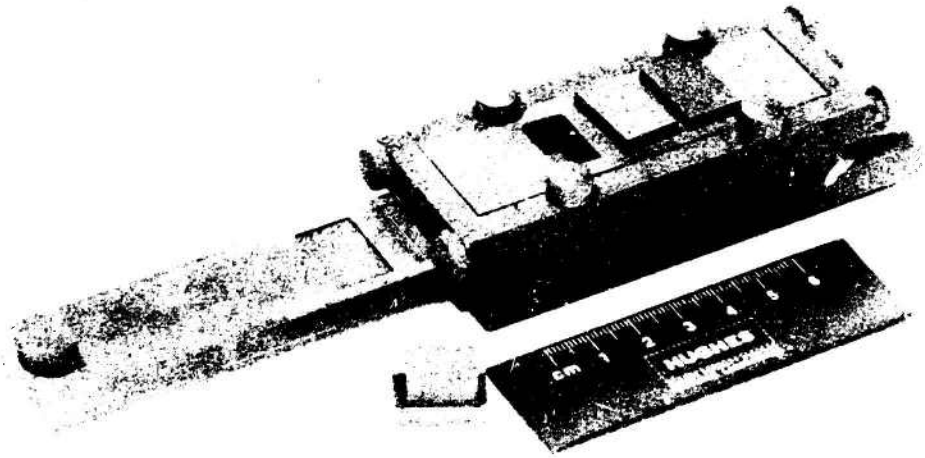

Fig. 9. Photograph of the Graphite Boat in which the Epitaxial Growth Occurs.

which are quite clean. At this time it is not clear whether the effect is due to a reduction in surface energy as the direct result of adding Al to the melt or to an increased tendency toward oxidation of the melt surface.

Another problem which was encountered in the growth of the initial GaAs films was that of thermal decomposition of the substrate during melt saturation. Besides pitting the surface to a depth of over a micron, thermal decomposition converts the surface layer of the substrate to p-type to a depth of several thousand angstroms. This leaves a troublesome interface layer between the film and the substrate.

This difficulty has been successfully eliminated by minimizing the time the substrate is exposed to high temperature and by supplying an equilibrium overpressure of arsenic during the high temperature period. The proper arsenic overpressure is achieved by placing a wafer of GaAs over the substrate when actual growth is not taking place.

At the end of GaAs growth experiments, growth occurred over the entire surface of a 1.5 cm^2 substrate even when the weight of the melt covering the substrate was less than 1.5 gm. Originally this was not possible since the surface tension of the melt causes it to ball up and wet only that part of the substrate directly beneath the ball. This tendency is now being defeated with a plunger type of melt cap which is made of high purity graphite and presses down on the melt, spreading it across the surface of the substrate. The use of small melt volumes is desirable in the growth of thin films since reproducibility in thickness then becomes consistent with practical temperature control capabilities.

(GaAl)As films have been grown in the system over the last 2 months both on GaAs and GaAlAs substrates. These films were grown with various compositions and thicknesses in order to ascertain our control capability. Thickness has been varied over the range of from 2 μm to 17 μm and composition from x = 0.02 to x = 0.25 ($Ga_{1-x}Al_xAs$). Complete evaluation of these films has not been made but preliminary inspection indicates good control over composition and average thickness but possible nonuniformity in thickness from point

to point on the thinner films (e.g., 2 μm). This has not been substantiated positively but initial staining experiments seem to indicate a reduction in film thickness toward the edges.

Another growth problem which remains to be resolved is the tendency for pyramidal growth to occur on the surface of the film at specific nucleation sites. These are few enough in number that their presence does not in itself produce problems; however, the graphite wiping edge breaks them off and scrapes them across the surface of the film leaving parallel scratches.

The elimination of thickness nonuniformity and scratching is our primary short-term program goal.

4. Characteristics of (GaAl) As Films

(GaAl)As films which have been grown thus far have been characterized through simple microscopic examination, staining cleaved cross sections, mechanical measurement of surface roughness (Dek-tak), measurement of avalanche breakdown voltage and microprobe examination (x-ray fluorescence).

Figure 10 is a photomicrograph of a typical thick (GaAl)As epitaxial film surface taken at low magnification (6X). The upper region of the substrate was not placed in contact with the melt and, consequently, has no epitaxial film. The horizontal line is, therefore, the edge of the film.

Several of the anomalies mentioned above are visible in this figure. Notice the vertical scratches originating at growth pyramids on the film. The scratches are in the direction the wiping edge was pulled across the surface.

Notice also the exaggerated thickness near the upper edge. This is due to incomplete removal of the melt in regions where the melt remains during the cool down to room temperature. In these regions growth continues leaving coarse crystalline deposits.

The gentle undulation of the surface is characteristic of thick films grown by the method described above. Figure 11 illustrates the magnitude of the surface undulation. The measurement was made with a Sloan Dek-tak. Notice that the average deviation from flatness of the surface is about ±1500 Å. This measurement was made on the 17-μm-thick film shown in Fig. 10. Thin films are, of course, much flatter.

The variation in Al concentration across a 5° beveled surface of the film in Fig. 10 was measured using x-ray flourescence. The results indicate that x varies from 4.21% at the substrate-epi interface to 3.57% at the surface of the film. This is the variation predicted by eq. (14) since the film is 17 μm thick and was grown with $(W_{melt}/A) = 1.5\ gm/cm^2$.

Thus far, all of the (GaAl)As films have been n-type with carrier concentrations on the order of a few times $10^{17}/cm^3$ as determined through measurement of available breakdown voltage. This is expected since we have been saturating the gallium solution with GaAs which is doped to $2 \times 10^{18}/cm^3$ with silicon. Because the distribution coefficient of Si at $900^{\circ}C$ in a gallium solution saturated with GaAs is about unity, it is expected that the silicon content of the grown layer will be about equal to the concentration of silicon in the source GaAs times the atom fraction of GaAs in the melt (≈0.1). In the future low doped films will be grown to reduce optical losses.

Thin layers about 2 μm thick have been grown on (GaAl)As substrates. These layers appear to be specularly flat although scratching is still a problem. Figure 12 is a photo micrograph of the cleaved edge of a 2 μm thick film of $Ga_{0.98}Al_{0.02}As$ on a 15 μm thick epi film of $Ga_{0.96}Al_{0.04}As$ purchased from Laser Diodes, Metuchen, New Jersey. The sample was stained with 1:3:4:2 ($HF: HNO_3: H_2O: H_2O_2$) to expose the different layers. The uniformity of thickness and composition of these thin layers is now being investigated.

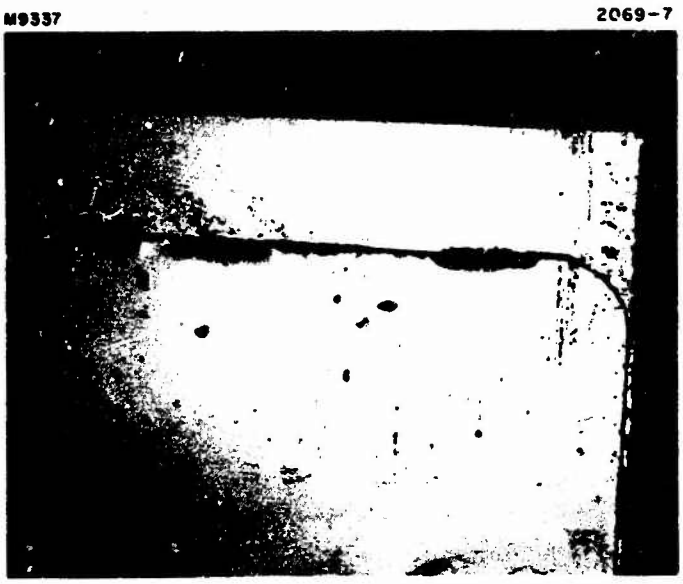

Fig. 10.
Photograph of the Surface of a (GaAl)As Film.

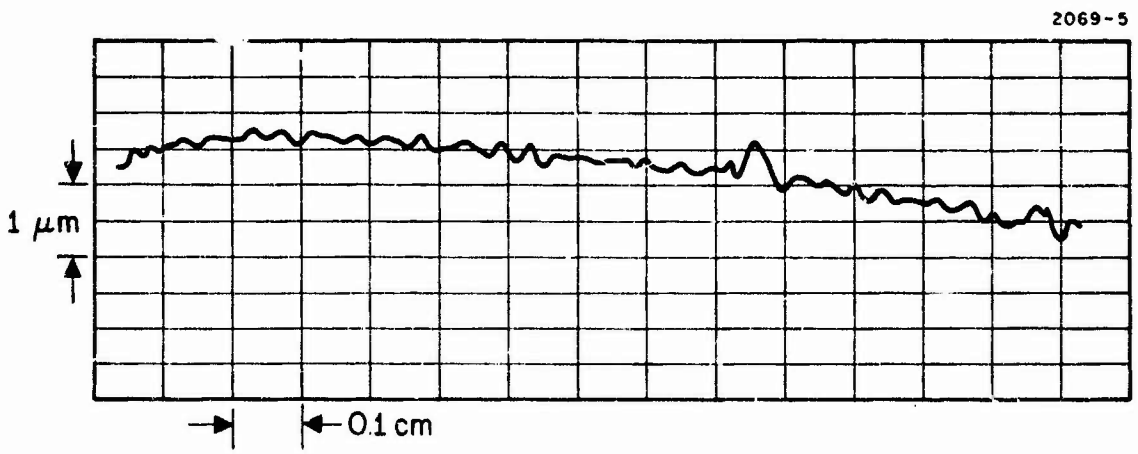

Fig. 11. Deviation in Surface Flatness of the Film Shown in Fig. 10.

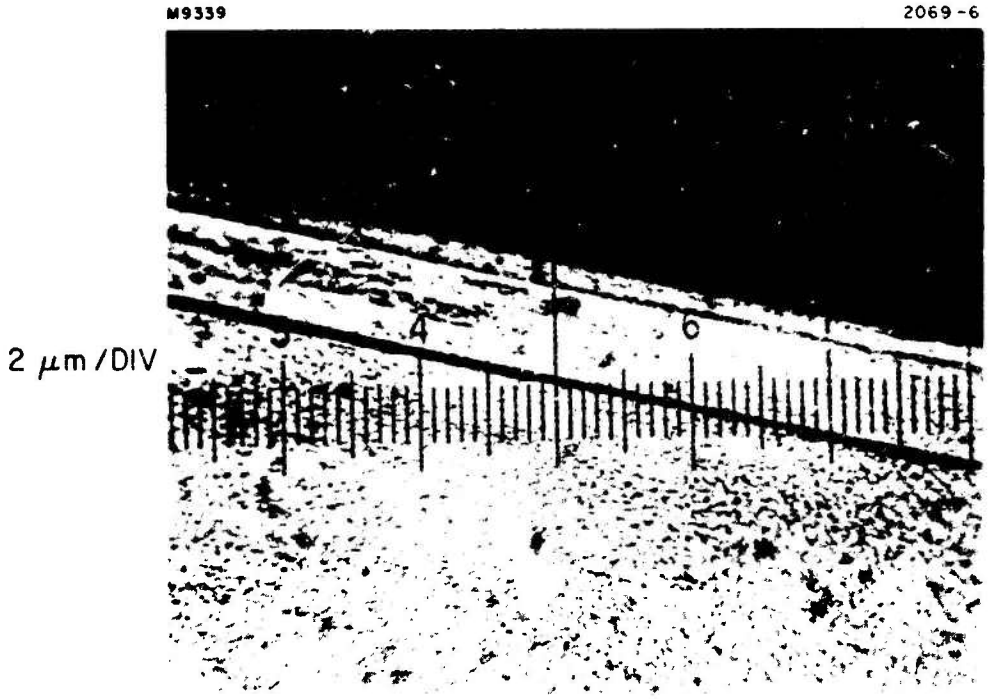

Fig. 12. Photomicrograph of the Cleaved Edge of a Double Layer of (GaAl)As on GaAs: Top Layer is $Ga_{0.98}Al_{0.02}As$ (3 μm Thick); Lower Layer is $Ga_{0.96}Al_{0.04}As$ (13 μm Thick); Substrate is GaAs.

SECTION IV

SEMICONDUCTOR FILM CHARACTERIZATION-PHOTOLUMINESCENCE MEASUREMENTS

Some of the film characterization work performed to date has already been described in Section III. This work included microscopic examination, staining of cleaved cross-sections, measurement of surface roughness, measurement of avalanche breakdown voltage, and x-ray fluorescence. In this section we describe an experimental setup which has been assembled for measuring the photoluminescence spectra of GaAs and $Ga_{(1-x)}Al_xAs$.

We intend to use photoluminescence measurements to analyze the quality of GaAs and $Ga_{(1-x)}Al_xAs$ epitaxial layers and the ratio of Ga/Al in the $Ga_{(1-x)}Al_xAs$. Such measurements provide a powerful tool for the detection of optically active centers produced by either contaminant atoms or crystalline defects in the material. The technique consists of optically "pumping" the material with relatively short wavelength radiation (6328 Å in our case) and observing and spectrally analyzing the emitted longer wavelength radiation. The peak emission wavelengths associated with optically active centers in GaAs have been extensively catalogued[4] generally making the photoluminescence technique a highly useful analytical tool. There are some limitations to using photoluminescence measurements, however. One of these is that the absorption coefficient in GaAs for light of wavelength shorter than 9000 Å is on the order of 10^5 cm^{-1}, meaning that the penetration depth is on the order of 0.1 μm. In order to analyze layers of greater thickness one must use some sort of layer "stripping" technique. However in some cases the limited penetration depth may be an advantage in that it provides depth resolution for concentration profile measurements.

Another limitation to photoluminescence measurements is that not all defect centers are detectable from light emission at a characteristic wavelength, since many defects act as nonradiative recombination centers. If such centers are present in high concentration they may

largely quench the radiation from other optically active centers. For example this is what occurs in layers that have been ion-implanted at room temperature or below and have not been annealed. In general, while the effect of nonradiative recombination must be considered in a photoluminescence analysis, it does not prevent the use of the method to analyze crystalline layers.

An experimental setup has been assembled for measuring the photoluminescence spectra of GaAs and $Ga_{(1-x)}Al_xAs$ as shown in Fig. 13. The optical pumping source is a 100 mW He-Ne laser with an output wavelength of 6328 Å. The samples are held in a vacuum dewar on the cold surface of a liquid nitrogen cryostat so that they can be cooled to 77°K if desired. Light emitted from the sample is collected by a lens and focused onto the slit of a Jarrell Ash 1/4 meter grating spectrometer. Specular reflections of the pumping laser light are directed away from the entrance slit by adjusting the angle between the sample and the laser beam, while diffusely scattered laser light which is collected by the lens is filtered out using a glass filter. The detector is a 7102 photomultiplier tube, which is cooled to reduce noise. The light passes through a rotating wheel chopper before entering the spectrometer so that the output signal from the phototube can be processed by a lock-in amplifier driving a chart recorder.

The photoluminescence measurement setup is presently being tested and "debugged" in preparation for use in evaluation of epitaxially grown films.

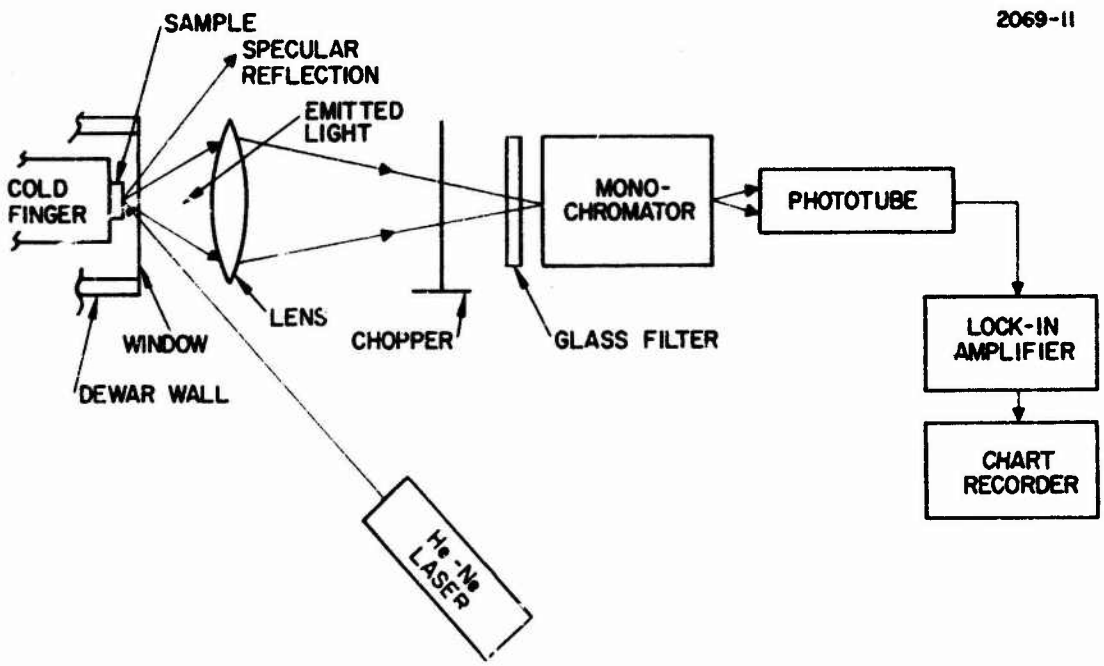

Fig. 13. Diagram of Photoluminescence Measurement Setup.

SECTION V

DEVICE ELEMENTS – APPLICATION OF ION MICROMACHINING TO THE FABRICATION OF THREE-DIMENSIONAL OPTICAL WAVEGUIDES

Experiments were carried out on determining the suitability of ion milling in fabricating three-dimensional ridge waveguides as well as optical directional couplers. These techniques should play an important role in the latter part of the program when integrated optics components will be fabricated. The HRL contribution to this phase of the program, namely fabrication by ion micromachining, has so far been Company supported.

A variety of thin films suitable for optical waveguiding has been reported so far. These include epitaxial layers of high resistivity on low resistivity GaAs, composite structure of GaAs-GaAlAs,[5] composite structure ADP-KDP,[6] and single crystal garnet films.[7] These layers can be grown with a high degree of purity and offer the attractive feature of being suitable for modulation.[5, 8] However, all these layers confine the light in one dimension only, and therefore as such are not compatible with the concept of optical circuitry.

To form a channel waveguide in which the radiation is confined in the two dimensions perpendicular to the direction of propagation, it is possible in some cases to use ion implantation[9] or diffusion.[10] We have been investigating the possibility of fabricating a channel guide by removal of superfluous sections of the epilayer (as shown in Fig. 14) by ion machining. The results of this work are described below. We also report here some preliminary measurements in a multimode directional coupler fabricated using this technique. Another important application of the technique is the fabrication of smooth and sharp terminations of channel guides. These terminations can be used for coupling in and out of the guide (either with a lens or directly with a fiber), or as mirrors to form resonators in samples that do not cleave easily.

Preceding page blank

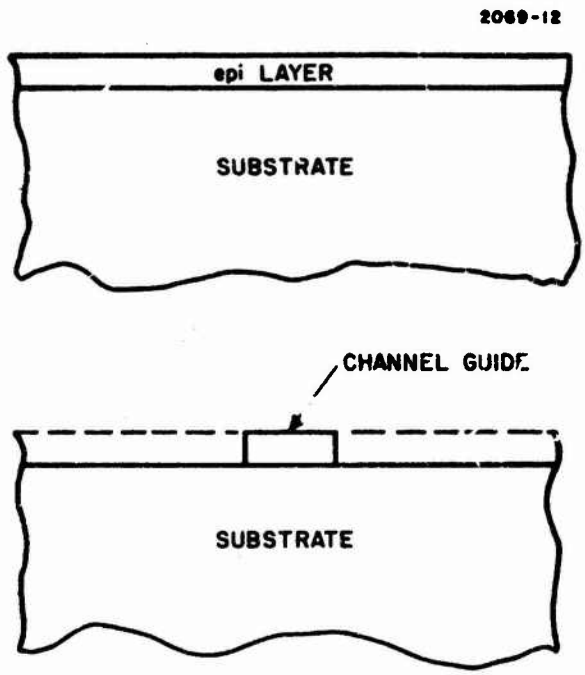

Fig. 14.
Channel Waveguide Fabrication by Removal of Superfluous Sections of an Epilayer.

The sputtering process provides a convenient method for thin film deposition and removal which can be applied to a wide variety of materials. The term sputtering refers to the ejection of atoms from a target surface by bombardment with energetic particles (usually ions with energies in the range of 0.6 to 20 keV). The ejected atoms can be either removed from a target substrate or deposited on an opposing substrate. Plasma sputtering is widely used in the microelectronics industry and has also been used in the fabrication of glass waveguides.[11] The plasma is usually created in an inert gas (at 10^{-1} to 10^{-3} Torr) by a ac or rf discharge and the sputtering occurs by ion bombardment from the plasma. Ion beam sputtering is performed by bombarding the target surface with a collimated ion beam in high vacuum. This type of sputtering has proved to be a useful alternative in instances where high vacuum conditions are desired for film deposition, or when control and direction of micromachining is important.[12]

For fabrication purposes an inert gas ion beam is produced in a duo-plasmatron-type ion source (as shown in Fig. 15), accelerated through a high vacuum chamber and directed (with or without final focusing) to impinge on a target surface. The high energy (typically 3 to 10 keV) impact of the ions causes sputtering ejection of the target material. By means of contact masking or by shadow masking, patterns can be machined (milled) into the surface of the target. The directed beam permits etching of patterns which are more sharply defined than those of chemical etching and, because no material is impervious to the sputtering attack, high resolution patterns can be produced in a broad variety of thin film materials.

A broad ion beam bombarding a target is used to accomplish high vacuum deposition of the sputtered target material onto an opposing substrate. This is illustrated by the alternate substrate position shown in Fig. 15. Electrons provided by the neutralizing filament are trapped in the potential of the ion beam and are available for continuous neutralization of any positive surface charge which may tend to accumulate. Therefore, dc bombardment suffices for sputtering deposition or removal of either metallic or insulating materials.

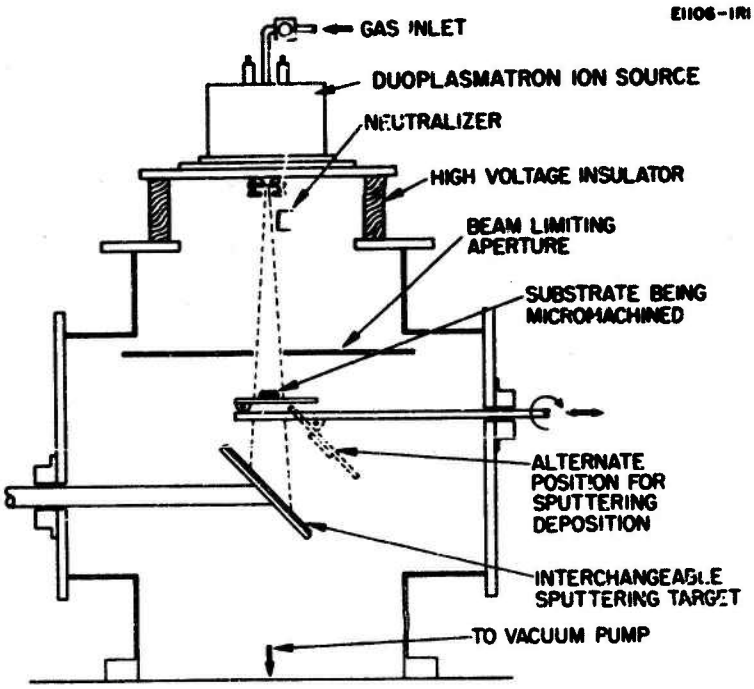

Fig. 15.
Schematic Diagram of the Duoplasmatron Ion Beam Sputtering System.

Since the back-sputtering rate proceeds uniformly in a given homogeneous material, the three-dimensional shape of a contact mask will be fairly well replicated in the substrate if sputtering continues until the mask is just etched away. Some distortion of the cross-sectional detail occurs because the sputtering rate varies with the angle of incidence. Also, the depth of etching into the substrate may differ from the depth of the photo-resist removed if the sputtering yields of the two materials differ.

We have investigated specifically the feasibility of applying ion milling techniques to the fabrication of channel waveguides in GaAs. The motivation for this investigation is derived from the eventual need to fabricate a large number of parallel optical channels in a single structure and from the desire to investigate the feasibility of fabricating optical directional couplers where it is necessary to have two waveguides in very close proximity. Of special interest are the smoothness of the "milled" guides and the dependence of the mode losses on the surface smoothness.

The channel illustrated in Fig. 14 is usually a multimode waveguide because of the large dielectric discontinuities on both sides. In principle the number of modes can be reduced to a desired number by choosing the appropriate substrate-epi dielectric discontinuity or by covering the guide with an appropriate index material. Because of the large dielectric discontinuity the scattering losses in the guide are very sensitive to the smoothness of the walls and the top surface. An extreme case of rough walls and top surface is shown in Fig. 16. This guide (3μ high, 7μ wide) scattered away most of the propagating light in a sample less than 1 mm long.

Much better results were achieved by using a thicker layer of photoresist (in order to protect the top surface), a better quality mask prepared by holographic techniques (details are given in Ref. 13), and by tilting the sample at various angles with respect to the bombarding ion beam during the machining. The result is shown in Fig. 17. The channel is 1.4μ high and about 2μ wide. A careful investigation of the losses in this kind of channel guide is under way.

M9387

Fig. 16.
An Extreme Example of a Guide with Rough Walls and Top Surface.

M9388

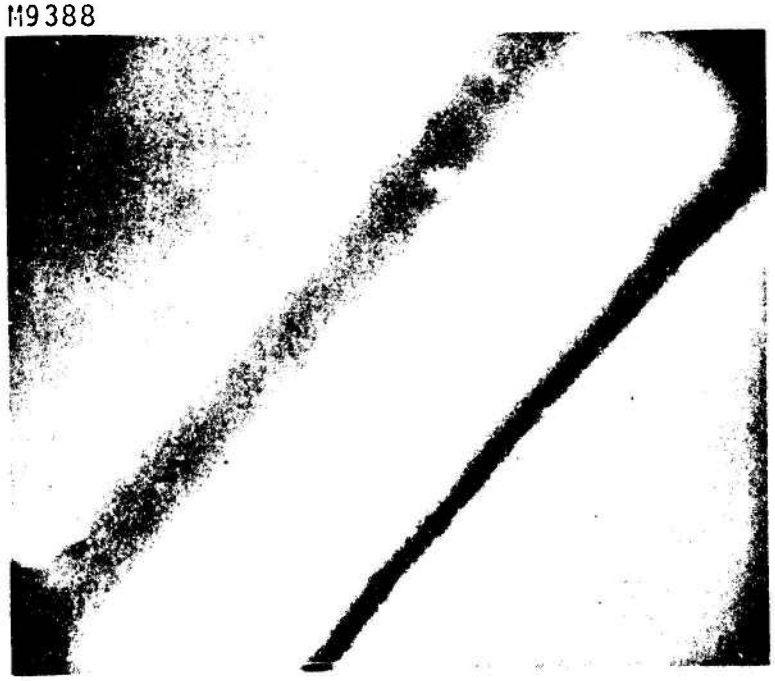

Fig. 17.
Good Quality Chanrel Waveguide Fabricated by Using Holography.

Directional couplers made of single mode waveguides embedded in the surface of GaAs have been fabricated by ion implantation.[9] In this case the coupling between two adjacent guides is caused by the overlap of the propagating modes as shown in Fig. 18a. Figure 18b shows the waveguides described earlier, in which the mode is very well confined in the x direction (because of the large dielectric discontinuity) and two closely spaced guides will thus have a negligible coupling. To increase the coupling between the guides, only a partial removal of the epilayer between them was performed as shown in Fig. 18c. Figure 19 is a preliminary measurement of the coupling. Figure 19a shows the cross section of an epilayer (about 8μ thick) that was machined down to the substrate, to form a large number of isolated channels. Light coupled into one channel emerges at the other end of the sample from that channel only (bottom photograph). However, when the same epilayer is only partially machined (Fig. 19b), light coupled into one guide emerges from three guides. Directional couplers of this sort can be used, for example, in tapping a multimode waveguide.

The sharp and smooth walls of the guide fabricated by ion machining and shown in Fig. 17 points to another important application of the technique. In some materials which do not cleave very well it is difficult to couple light into channel guides because of edge roughness. (Prism and grating couplers are suited mainly for two dimensional guides and coupling into a channel guide is done usually by focusing a beam with a lens or by attaching a fiber to the channel edge). Thus, terminating an embedded or ridged channel guide by ion machining can yield a smooth edge and efficient coupling. Since parallel cleaves are used in semiconductor lasers as mirrors, it is possible to form this kind of mirror by ion machining. Mirrors fabricated by this technique do not have to be flat and can be curved in order to increase cavity Q.

The high quality of the machining required for integrated optics components calls for the use of a scanning electron microscope for

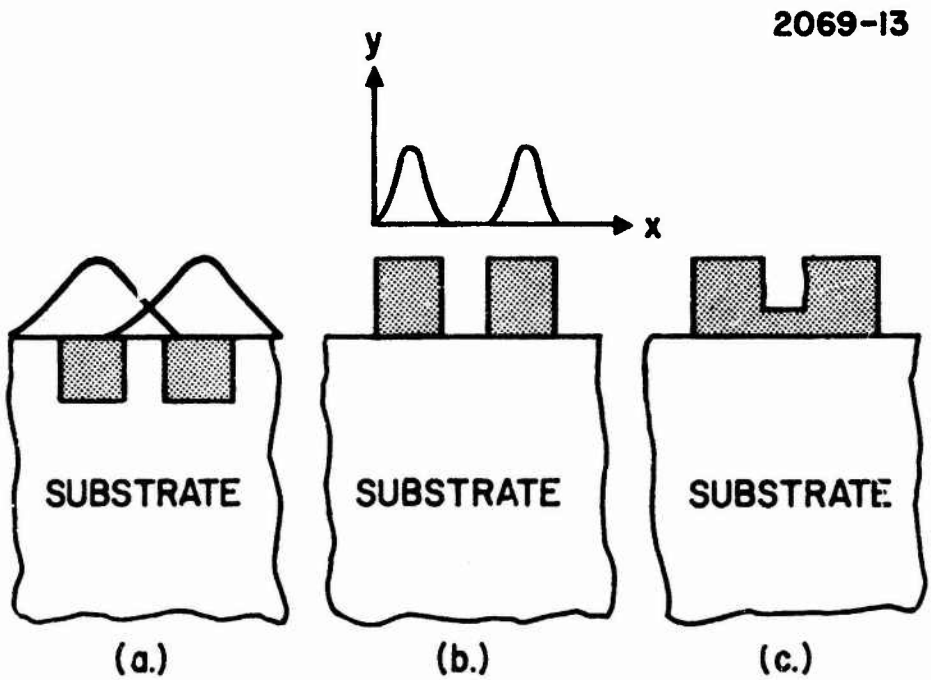

Fig. 18.
Directional Couplers Fabricated in GaAs. (a) Single Mode Directional Coupler fabricated by Ion Implantation. (b) Two Isolated Channel Guides with No Coupling. (c) Two Channels with Increased Degree of Coupling.

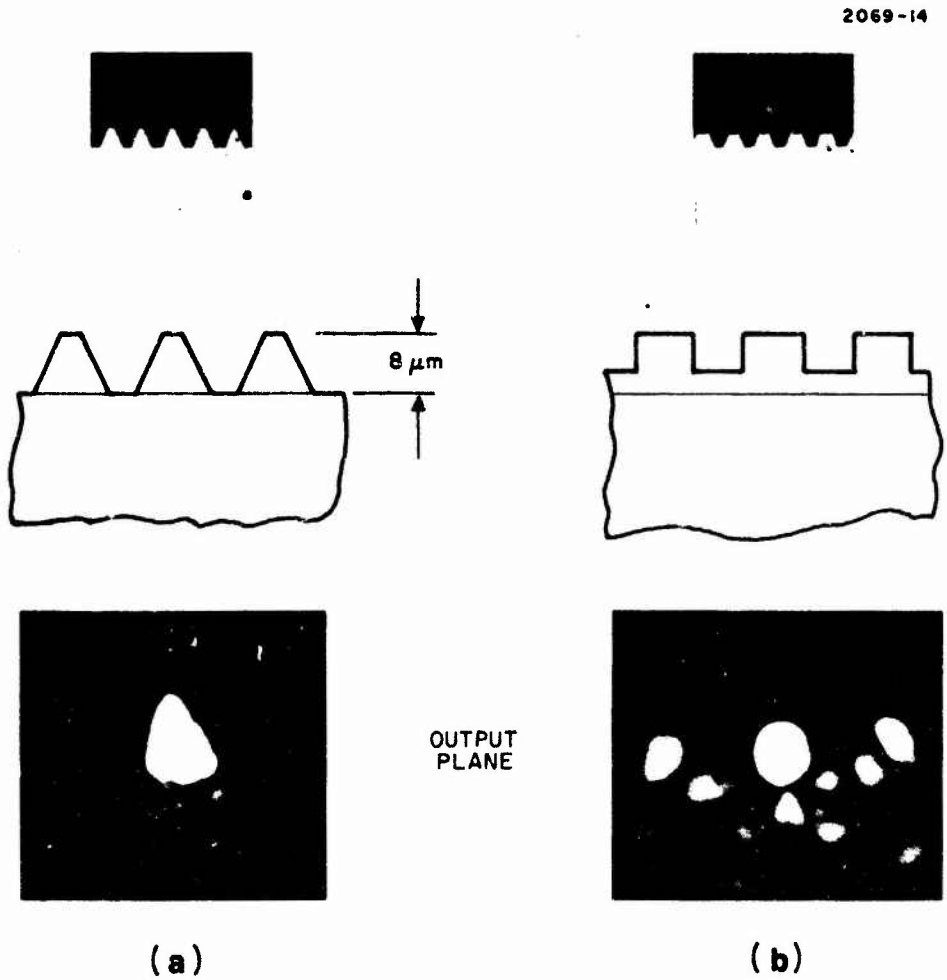

Fig. 19. Multimode Directional Coupler Fabricated by Ion Machining in a GaAs Epilayer. (a) Isolated Channels. (b) Coupled Channels.

examination of devices and for the production of masking patterns when the dimensions are less than one micrometer. The high resolution capability of SEM[14] should play an important role in future integrated optics applications.

SECTION VI

FUTURE PLANS

The success we have had in using our simple model for liquid epitaxial growth leads us to believe that in a short time we can make rapid progress toward producing waveguide structures using thin films of GaAlAs of varying composition in a controlled way. This aspect of the program which uses the horizontal open tube growth method will have a high priority in the near future. Multiple layer films of $Ga_{1-x}Al_xAs$ of varying composition satisfactory for use as waveguides will be grown in the next period. Attention will be paid to purity in starting materials to minimize absorption losses. Details of the growth system will be investigated to reduce pyramid growth and scratches resulting from this growth.

The theoretical model we have used also indicates that there are advantages to be gained by using large melts to obtain more homogeneous films. We intend to use our vertical dipping system to grow simple layers of GaAlAs on substrates of slightly different composition to evaluate such an approach.

When good substrate layers with controlled composition of GaAlAs become available from the liquid epitaxy methods, we intend to use these to grow pure GaAs layers to be used as waveguides.

Photoluminescent bandgap measurements will be made on a variety of compositions of $Ga_{(1-x)}Al_{(x)}As$ films and compared with Ga/Al ratios determined from electron microprobe results.

As material becomes available, the optical propagation characteristics such as loss, dispersion and field profiles of the films will be measured. Subsequent to this, device structures of various types will be fabricated and their performance characteristics determined. Experimental setups to perform the above mentioned measurements are presently available.

REFERENCES

1. N. G. Spitzer, et al (Phys. Rev. 14, p. 59, 1959).

2. R. N. Hall, "Solubility of III-V Compound Semiconductors in Column III Liquids," Journal of Elec. Chem. Soc., 385-388 (May 1965).

3. J. M. Blum and K. K. Shih, "The Liquid Phase Epitaxy of $Al_xGa_{1-x}As$ for Monolithic Planar Structures," Proc. of IEEE, 59, 1498-1502 (October 1971).

4. "Semiconductors and Semimetals - Vol. 8 Transport and Optical Phenomena," Edited by R. K. Willardson and A. C. Beer, Academic Press (1972), Chapter 5.

5. A. Yariv, Proceedings of 1971 Esfahan Conference on Pure and Applied Quantum Electronics (J. Wiley, in press). Also, F. K. Reinhart, B. I. Miller, "Efficient GaAs - $A\ell_xG_{al-x}As$ Double-Hetrostructure Light Modulators," Appl. Phys. Letters 20, 36 (1972).

6. V. Ramaswamy, "Epitaxial Electro-Optic Mixed Crystal $(NH_4)_xK_{1-x}H_2PO_4$ Film Waveguide," Appl. Phys. Letters, 21, 183 (1972).

7. P. K. Tien, R. J. Martin, S. L. Blank, S. H. Wemple, and L. J. Vernerin, "Optical Waveguides of Single-Crystal Garnet Films," Appl. Phys. Letters, 21, 207 (1972).

8. P. K. Tien, R. J. Martin, R. Wolfe, R. C. LeCraw, and S. L. Blank, "Switching and Modulation of Light in Magneto-Optic Waveguides of Garnet Films," Appl. Phys. Letters 21, 394 (1972).

9. S. Somekh, E. Garmire, A. Yariv, H. L. Garvin and R. G. Hunsperger, "Channel Optical Waveguide Directional Couplers," Appl. Phys. Letters 22, 46 (1973).

10. W. E. Martin and D. B. Hall, "Optical Waveguides by Diffusion of II-VI Compounds."

11. J. E. Goell and R. D. Standley, "Sputtered Glass Waveguides for Integrated Optical Circuits," BSTJ, Vol. 48, pp. 3445-3448, December 1969.

Preceding page blank

12. H. L. Garvin, "Ion Beam Sputtering for Thin Film Deposition and High-Precision Micromachining," Proc. 3rd. Symposium on the Deposition of Thin Films by Sputtering, Rochester, N. Y. (Sept. 7-10, 1969), pp. 4-11.

13. H. L. Garvin, E. Garmire, S. Somekh, H. Stoll, and A. Yariv, "Ion Beam Micromachining of Integrated Optics Components," to be published in Applied Optics (March 1973).

14. E. D. Wolf, et al., "Response of Elvacite 2041," Proc. 11th Symposium on Electron, Ion and Laser Beam Technology, Boulder, Colorado, 1971.

APPENDIX

CALCULATION OF FREE CARRIER ABSORPTION

The equation of motion of an impurity electron can be written as

$$- \omega^2 m^* x + \frac{i\omega m^* x}{\tau} = -e\, E\, e^{i\omega t}$$

where

m^* = effective mass

τ = scattering time

E = electric field amplitude

From the solution of this equation we obtain,

$$x = \frac{-eE/m^*}{-\omega^2 + i\omega/\tau}$$

$$D \equiv \epsilon_{total} E = \epsilon E + P_{electr} = \epsilon E + Nex$$

$$\epsilon_{total} = D/E = \epsilon \cdot \frac{Ne^2/m^*}{\omega^2 + 1/\tau^2} - i \frac{\frac{Ne^2\omega}{m^*\tau}}{\omega^4 + \omega^2/\tau^2}$$

$$\epsilon_{total} = \epsilon_o \left(K_r^P - \frac{Ne^2/m^*\epsilon_o}{\omega^2 + 1/\tau^2} - i \frac{Ne^2/(m^*\epsilon_o\omega\tau)}{\omega^2 + 1/\tau^2} \right)$$

where, K_r^P is the real part of the relative dielectric constant for the material with no impurities.

Therefore,

$$\mathrm{Im}J_{\cdot} = -\frac{Ne^2 (m^* \epsilon_o \omega\tau)}{\omega^2 + 1/\tau^2}$$

For a wave propagating as

$$\exp(i\omega t - ikz)$$

we have

$$k = \omega\sqrt{\mu_o \epsilon_{total}}$$

$$\approx \omega\sqrt{\mu_o \epsilon}\left(1 - \frac{Ne^2}{2m^* \epsilon \omega^2} - i\,\frac{Ne^2}{2m^* \epsilon \omega^3 \tau}\right) \qquad \text{A-1}$$

where we assumed $\omega^2 \gg 1/\tau^2$. The power absorption coefficient is, therefore, given by

$$\alpha = 2\,(\mathrm{Im}K) = \frac{k_o K_i}{\sqrt{K_r}} = \sqrt{\frac{\mu_o}{\epsilon}}\,\frac{Ne^2}{m^* \omega^2 \tau}\ .$$